

# Anatomizing Exotic Production of the Higgs Boson

Felix Yu\*

*Theoretical Physics Department, Fermilab, Batavia, IL 60510, USA*

We discuss exotic production modes of the Higgs boson and how their phenomenology can be probed in current Higgs analyses. We highlight the importance of differential distributions in disentangling standard production mechanisms from exotic modes. We present two model benchmarks for exotic Higgs production arising from chargino-neutralino production and study their impact on the current Higgs dataset. As a corollary, we emphasize that current Higgs coupling fits do not fully explore the space of new physics deviations possible in Higgs data.

arXiv:1404.2924v1 [hep-ph] 10 Apr 2014

---

\* felixyu@fnal.gov

## I. INTRODUCTION

While the importance of the discovery of the Standard Model (SM)-like Higgs boson by the CMS and ATLAS experiments [1–6] cannot be understated, many experimental tests remain in order to determine whether the new particle is truly the Standard Model Higgs boson. Correspondingly, searches for non-Standard Model-like properties of the new particle are highly motivated, especially since a natural solution to the gauge hierarchy problem invariably leads to deviations in the couplings of the Higgs boson to SM states [7]. So far, coupling extractions done by both theorists [8–27] and experimentalists [28–32] have concluded overall consistency with a purely SM Higgs boson. Further studies of the spin properties [33–38] have corroborated the SM-like nature of the new boson. Nevertheless, these coupling fits admittedly require model assumptions about how separate analyses in different Higgs decay states are related. Crucially, the SM production mechanisms in these coupling fits are only deviated by changing their respective signal strengths. Our goal is to explore exotic production of the SM-like Higgs boson, characterize how exotic production modes can be differentiated from SM production modes, and quantify the extent to which current Higgs analyses can be contaminated by a new exotic production mode benchmark.

Our work strengthens the current and future of the LHC effort in extracting as much information as possible from the Higgs signal, including the Higgs discovery analyses from ATLAS [4–6, 39] and CMS [1–3, 40]. We provide an initial foray into the direct study of exotic production using the current Higgs analyses and are thus distinct from proposed improvements of Higgs production tests [41–48]. It is complementary to recent work on exotic decays of the Higgs boson [49, 50], which already have experimental limits in a small number of channels, most notably the possible invisible decay of the Higgs boson to dark matter candidates [51–54]. In contrast, while probes of new exotic decays typically require dedicated analyses, exotic production modes of the Higgs are probed by kinematic distributions of the Higgs candidate and the other particles produced in association with the Higgs. These studies can be done with current data and minimal modification to current analyses and may reveal hints of a new exotic production mode for the Higgs boson. Such studies are vitally important in testing whether Higgses at the LHC arise only from SM production modes.

In this letter, we will demonstrate the viability and importance of models featuring exotic Higgs production. We will first discuss the general phenomenology of exotic production in Sec. II. We will then present benchmark models of chargino-neutralino production in the minimal supersymmetric standard model (MSSM), and discuss its phenomenology and the current experimental status

in Sec. III. In Sec. IV, we analyze how the new exotic mode will affect the Higgs discovery analyses and discuss the tests needed to disentangle SM and exotic production modes. We conclude in Sec. V. Auxilliary material derived from the Higgs discovery analyses is in Sec. A.

## II. PHENOMENOLOGY OF EXOTIC PRODUCTION OF THE HIGGS BOSON

The number of Higgs candidates in any given final state scales as

$$N_{\text{events}} = L\sigma\text{Br} \epsilon \sim \frac{g_p^2 g_d^2}{\Gamma}, \quad (1)$$

where  $L$  is the integrated luminosity,  $\sigma$  is the production cross section,  $\text{Br}$  is the appropriate branching fraction,  $\epsilon$  is the signal efficiency,  $g_p$  is the production coupling of the Higgs,  $g_d$  is the decay coupling of the Higgs, and  $\Gamma$  is the total Higgs width. For the Higgs resonance, since the Higgs width is too narrow to be identified directly<sup>1</sup>, each final state only determines the combination of  $g_p^2 g_d^2 / \Gamma$ . Moreover, the production mechanism cannot be tuned at the LHC, and so multiple signal production modes typically contribute to a given final state analysis. The contamination from multiple production modes is well-known and can be mitigated by strict cuts. For example, the 2-jet category of the diphoton analysis is most suited to vector boson fusion production but can have 20% to 50% contamination from gluon fusion production [1, 4]. Knowing the efficiencies of how different production modes contribute to a given final state is critical in order to appropriately combine separate rate measurements and extract production and decay couplings. Thus far, exotic production modes have been neglected in these coupling scans, leaving open the possibility that current coupling fits are overinterpreting the Higgs dataset. We will demonstrate that exotic production modes are viable and characterize how their signatures differ from SM production modes.

Exotic production modes for the SM-like Higgs boson can arise from new physics models with heavy particles whose decay products include the 126 GeV Higgs. Familiar signatures of this type include new resonances in two Higgs doublet models, where the heavy  $CP$ -even Higgs scalar  $H$  can decay to a pair of light  $CP$ -even Higgses,  $H \rightarrow hh$ , or the  $CP$ -odd pseudoscalar  $A$  can decay to the SM  $Z$  boson and the light Higgs boson,  $A \rightarrow Zh$ . These have been recently searched for at CMS [59], excluding  $\sim \text{few pb } \sigma \times \text{Br}$  for resonances in the 260 to 360 GeV region.

Alternatively, new particles can produce cascade decays that could include Higgs bosons. Stops and gluinos in the MSSM, for example, can cascade decay to heavy neutralinos, which can then

---

<sup>1</sup> Indirect extraction of the Higgs width has been proposed, explored, and recently performed in Refs. [55–58].

decay to Higgs bosons and lighter neutralinos. Since these parent particles can be strongly produced, the MSSM rate for Higgs production could have been very large and exceed SM production rates. Moreover, these cascade decays of heavy superpartners have interesting phenomenological signals [60–63], including boosted Higgs signatures for the  $b\bar{b}$  channel [64–66]. The key players for exotic Higgs production in the MSSM, though, are typically the heavy neutralinos, and thus the strong production rates studied above are absent if new colored states are too heavy to be produced, as is currently favored by present data. Nevertheless, observable signals with weak scale cross sections are still interesting. Correspondingly, Drell-Yan chargino-neutralino production has been extensively studied [67–71] and recently revisited [72–87].

The cascade decay class of exotic production can be divided further into symmetric and asymmetric subcategories. Decay cascades giving Higgses from symmetric production, such as stop-anti-stop production from the MSSM, necessarily have a predicted correlation between single- and double-Higgs production. Namely,

$$\sigma_{h+X} = \sigma \times 2\mathcal{B}(1 - \mathcal{B}) , \quad (2)$$

$$\sigma_{hh+X'} = \sigma \times \mathcal{B}^2 , \quad (3)$$

where  $\sigma$  is the total cross section and  $\mathcal{B}$  is the overall decay chain branching fraction to a SM-like Higgs, assuming the decay chain does not produce multiple Higgs particles. This correlation implies strong constraints on symmetric exotic production models driven by current limits on double Higgs production. The current best searches for double Higgs production rely on the  $b\bar{b}\gamma\gamma$  final state [88], while the highest significance Higgs decay modes are the  $\gamma\gamma$ ,  $ZZ^* \rightarrow 4\ell$ , and  $WW^* \rightarrow \ell\nu\ell\nu$  analyses. The correlated rates for an exotic symmetric production mode in the single Higgs  $\gamma\gamma$  final state with the double Higgs  $b\bar{b} + \gamma\gamma$  final state are then

$$\sigma_{h+X} = \sigma \times 2\mathcal{B}(1 - \mathcal{B}) \times \text{Br}(h \rightarrow \gamma\gamma) , \quad (4)$$

$$\sigma_{hh+X'} = \sigma \times \mathcal{B}^2 \times 2\text{Br}(h \rightarrow \gamma\gamma)\text{Br}(h \rightarrow b\bar{b}) , \quad (5)$$

giving a single- to double-Higgs ratio  $\frac{1-\mathcal{B}}{\mathcal{B} \times \text{Br}(h \rightarrow b\bar{b})} \sim \frac{1-\mathcal{B}}{0.6\mathcal{B}}$ . For large values of  $\mathcal{B}$ , the effect on double Higgs rates would be larger than the added single Higgs rate, implying searches for double Higgs production are a better probe of such scenarios. Conversely, for small  $\mathcal{B}$ , the large non-Higgs decay rate implies the main search modes for such models would not be via Higgs final states. Of course, double Higgs analyses are insensitive to asymmetric cascade decay exotic production modes, and so asymmetric parent particle production is a particularly motivated class of exotic Higgs production.

Exotic production modes for the Higgs-like scalar exist in many beyond the standard model theories. Previous studies, however, largely neglected the regions of parameter space where the exotic production kinematics overlapped with SM production kinematics (an exception, though, is [89]). As we enter the era of precision studies of Higgs properties, it is thus timely and important to understand these previously unexplored regions of parameter space. Quantifying the extent of possible overlap between exotic and SM production will be a main result of this work.

Higgs production modes are distinguished by two classes of measurements: (1) kinematics of the Higgs candidate, and (2) kinematics and multiplicities of the objects produced in association with the Higgs. This is readily justified because of the narrow Higgs width and the scalar-like nature favored from spin studies, which allow the Higgs decay state kinematics to be calculated in the Higgs rest frame and then boosted according to the production mode kinematics. Inclusive Higgs rates, since they sum over contributions of several different production modes with different efficiencies, cannot disentangle the precise contribution of each contributing mode. On the other hand, exclusive measurements exercise binning by multiplicities of associated leptons and/or jets in the event to isolate particular production modes. Binning by jet and lepton multiplicity is already in use by the experiments to attempt to disentangle vector boson fusion (VBF), vector boson association (VBA) and gluon fusion (ggF) production modes. Yet, this is insufficient if new physics (NP) modes are also present, since these rates can only determine combinations of sums of production modes and their respective efficiencies. Different production modes are instead best tested using differential distributions of the Higgs candidates and the associated objects. These distributions, such as Higgs  $p_T$  and  $\eta$ , associated jet and lepton  $p_T$  and the event-level missing transverse energy (MET), readily constrain the rates and shapes of all production modes present in a given final state analysis. Cross correlations between orthogonal final states in related differential distributions will then test whether the production profile of the Higgs in one channel is consistent with other channels.

To this end, we motivate the simultaneous study of both rate information and differential distributions in order to anatomize the Higgs production modes. We will focus now quantifying how measured rates, which forms the basis for Higgs coupling fits, can be contaminated by additional exotic production modes.

### A. Higgs rates and exotic production

In the Standard Model, the main production mode for the Higgs boson at hadron colliders is gluon fusion, which dominates over the remaining vector boson fusion,  $W^\pm h$ ,  $Zh$ , and  $t\bar{t}h$  production modes. In this vein, additional subleading SM production modes, such as  $th$  or triple boson production including a Higgs, are neglected and, especially if they are enhanced by new physics, can be considered as exotic production modes. Moreover, while direct searches for new physics at the LHC have excluded some large regions of NP parameter space, only a limited number of direct searches consider final states that include Higgs bosons. As the Higgs boson may be the leading connection between SM and new physics sectors, it is worthwhile to consider that new physics first shows up in Higgs physics instead of the traditional dedicated NP analyses. Clearly, NP scenarios can thus be constrained from studies of Higgs rates: however, as mentioned before, such rates only constrain linear sums of various production modes and are thus not truly model-independent. Moreover, it is possible that SM production rates are reduced via NP effects [90], but exotic production is simultaneously present to make up any noticeable difference.

We can subdivide NP exotic production rates into three categories: (A)  $\sigma_{NP} \gtrsim \sigma_{SM}$ , (B)  $\sigma_{NP} \sim \sigma_{SM}$ , and (C)  $\sigma_{NP} \lesssim \sigma_{SM}$ , where  $\sigma_{SM}$  refers to the various calculated SM Higgs production cross sections. The high resolution  $\gamma\gamma$  and  $ZZ^* \rightarrow 4\ell$  channels from ATLAS [4, 5, 28–30] and CMS [1, 2, 31] give combined Higgs mass measurements of  $125.5 \pm 0.2$  (stat.) $_{-0.6}^{+0.5}$  (syst.) GeV [ATLAS] and  $125.7 \pm 0.3$  (stat.)  $\pm 0.3$  (syst.) GeV [CMS]. Approximating the Higgs mass as 126 GeV, we list the dominant SM production modes and their percentage uncertainties in Table I, taken from Refs. [91–93].

Mode	Cross section (pb)	QCD scale (%)	PDF+ $\alpha_s$ (%)
ggF	18.97	(+7.2, -7.8)	(+7.5, -6.9)
VBF	1.568	(+0.3, -0.1)	(+2.6, -2.8)
$W^\pm h$	0.6860	(+1.0, -1.0)	(+2.3, -2.3)
$Zh$	0.4050	(+3.2, -3.2)	(+2.5, -2.5)
$t\bar{t}h$	0.1262	(+3.8, -9.3)	(+8.1, -8.1)

TABLE I. From Ref. [93], SM Higgs production cross sections and theoretical uncertainties for the main production modes for 126 GeV Higgs at 8 TeV LHC.

Since current Higgs rates are roughly consistent with SM expectations, we find only category (B) is worthwhile for detailed study at present. Category (A) is viable if the NP signal efficiency is tiny,

which requires very non-standard kinematics (such as displaced vertices giving Higgs decays [94]), which would be better addressed by dedicated searches. Category (C) is also presently unmotivated, since the current experimental and theoretical uncertainties on Higgs rates are too large to possibly constrain additional exotic production modes that are subleading compared to SM rates. For category (B), knowing the signal efficiencies for various SM and NP production modes is key to understanding how sensitive rate analyses will be in disentangling NP from SM production, which is the focus of Sec. IV.

We could include another category of NP Higgs exotica, namely exotic decays of the Higgs boson (see, e.g. Refs. [49, 50]). We view the possibilities of exotic production modes and exotic decays of the Higgs, however, as complementary probes for understanding the connections between the Higgs and new physics. More practically, the phenomenology of exotic production and exotic decays require different tools. Probing exotic production requires a well-defined Higgs candidate and then analyzing the global event properties to test how it was produced. Exotic decays of the SM-like Higgs, however, require dedicated searches for new final states, where the exotic Higgs signal candidates must be isolated from background. In this work, we will only focus on exotic production, though combining exotic production and exotic decay signatures would be interesting for future study. Thus, we will assume the SM Higgs partial decay widths are not significantly modified by NP and that no new decay modes for the Higgs are introduced.

## B. Current sensitivity to exotic production

The experiments have done several searches for Higgs signatures, aiming to probe various final states and, to a separate degree, isolating particular production channels. We first discuss the overall status of Higgs measurements and then isolate the most relevant Higgs analyses that are sensitive to exotic production modes. We outline the searches below, critically evaluating each search and its sensitivity to exotic production signals.

The extent to which a new exotic production mode is categorized in the current experimental searches is best understood by differentiating exclusive and inclusive Higgs production searches. More inclusive Higgs searches, such as the diphoton, fully leptonic  $ZZ^*$  channel, fully leptonic  $WW^*$  channel, and  $\tau\tau$  analyses from ATLAS [4–6, 39] and CMS [1–3, 40] use cuts on jets, leptons, and missing energy in order to partition the contributions of separate SM production modes. Other searches singly target vector boson fusion production [95, 96], vector boson associated production [97–102], or  $t\bar{t}h$  production [103–106]. While each result standalone can readily be interpreted

as an observed experimental rate, the combination of separate searches relies crucially on assumptions about the underlying production modes and is hence altered when a new exotic mode is considered. As mentioned before, the combinations from ATLAS [28–30] and CMS [31] do not consider possible contamination of the Higgs dataset from exotic production modes. In order to determine the extent and constraints on new exotic production modes, the rates, kinematics and multiplicities of associated objects, and the kinematics of the Higgs candidate must all be measured and given. In addition, the efficiencies for the exotic production mode must be simulated in order to know how the new mode is tagged and possibly disentangled from the SM modes.

In principle, any new putative exotic Higgs production mode must be considered in all possible Higgs decay final states. The most important analyses for our purposes, however, are the  $\gamma\gamma$ ,  $ZZ^* \rightarrow 4\ell$ , and  $WW^* \rightarrow \ell\nu\ell\nu$  measurements, since these analyses make the most use of event categorization based on objects produced in association with the Higgs. Other final states, such as  $\tau\tau$  and  $b\bar{b}$ , have less sensitivity to the SM Higgs production rates with current data, and are expected to be less powerful in disentangling new production modes unless the exotic mode itself is rich in  $\tau$  or  $b$  production. Singly targeted analyses for SM VBF, VBA, or  $t\bar{t}h$  production, if they do not categorize according to expected SM production contributions, each measure only a single rate. Hence, their impact beyond the discovery modes is minimal, since the expected cross correlations from a new exotic production mode in separate categories should already be present in the discovery modes. Thus, we focus our attention on the Higgs discovery modes of  $\gamma\gamma$ ,  $ZZ^* \rightarrow 4\ell$ , and  $WW^* \rightarrow \ell^+\nu\ell^-\nu$  final states. These have the additional advantage of being very cleanly measured final states, and so further analyses of differential distributions are highly promising and well-motivated<sup>2</sup>. While this has been done by ATLAS in the  $\gamma\gamma$  channel [108], we look forward to future presentations of differential distributions by ATLAS and CMS, possibly including the  $4\ell$  final state.

We can see that a well-motivated and timely scenario for further study is characterized by cross sections similar to SM production rates and regions of parameter space where the exotically produced Higgs has kinematics similar to SM kinematics. Moreover, to readily avoid constraints on double Higgs production, it is simplest to consider asymmetric production of parent particles that cascade decay to a Higgs in the final state. Surveying possible exotic production modes, we now consider chargino-neutralino production in the MSSM as a well-motivated benchmark for studying exotic production.

---

<sup>2</sup> Also advocated in Ref. [107].

### III. CHARGINO-NEUTRALINO PRODUCTION IN THE MSSM

In the minimal supersymmetric standard model, there are many possible cascade decay chains that produce Higgs bosons. Squarks, for example, can decay to Higgs bosons via flavor-conserving heavy to light flavor decays. Neutralinos and charginos, via mixing, can decay to Higgs bosons in transitions from heavy to light mass eigenstates. We will focus on the cascade decay of a heavy neutralino into a light neutralino and the SM-like Higgs boson.

Chargino-neutralino production at the LHC dominantly proceeds via an  $s$ -channel  $W^\pm$  boson, and assuming simple two-body decays of the chargino and neutralino, leads to the final state of  $W^\pm h \chi_1^0 \chi_1^0$  or  $W^\pm Z \chi_1^0 \chi_1^0$ , as shown in Fig. 1. If the  $W^\pm h$  cascade decay is favored over the  $W^\pm Z$  cascade decay, then the  $\chi_1^\pm \chi_2^0$  production will not be seen in traditional multilepton searches and will instead be probed by Higgs exotic production searches. The important parameters in determining these relative rates are the electroweak gaugino mass terms,  $M_1$ ,  $M_2$ ,  $\mu$ , and  $\tan\beta$ . The first three, apart from potentially significant mixing effects, determine the bino, wino, and higgsino masses. After  $SU(2)$  breaking, the bino, neutral wino, and two neutral higgsino states mix, and the charged wino and charged higgsino mix.

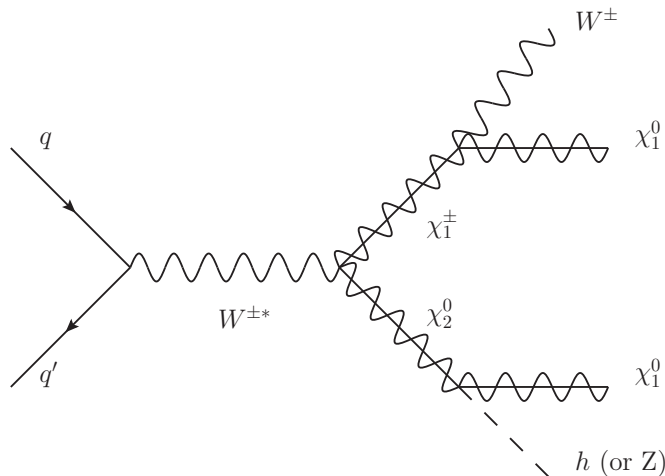


FIG. 1. Feynman diagram for  $\chi_1^\pm \chi_2^0$  production.

The tree level interactions between neutral gauginos in the gauge basis are easy to identify. There are diagonal  $Z$  mediated interactions for  $\tilde{H}_d^0$  and also for  $\tilde{H}_u^0$ . After mixing, the particular combination of gauge eigenstates given by  $\frac{1}{\sqrt{2}}(\tilde{H}_d^0 \pm \tilde{H}_u^0)$  can exchange  $Z$  bosons between each other but do not have diagonal  $Z$  couplings. Separately, Higgs exchange only exists between Higgsino eigenstates and gaugino eigenstates. So, while pure neutral winos and pure binos have

no tree-level vertices amongst themselves, wino-like neutralinos can decay to Higgses and bino-like neutralinos via a Higgsino mixing angle insertion, while a  $Z$ -mediated decay requires two Higgsino mixing angles. Because of possible intrinsic cancellations among up and down Higgsino mixing angles, however, the  $Z$ -mediated decay may still dominate. A more extensive discussion of the relative branching fractions of next-to-lightest supersymmetric particles (NLSPs) is available in Ref. [84], but we can simplify the parameter space to variations in  $\mu$  and  $M_2$ , holding  $M_1$  and  $\tan\beta$  fixed.

In Fig. 2, we show that  $\text{Br}(\chi_2^0 \rightarrow h\chi_1^0)$  can readily dominate over  $\text{Br}(\chi_2^0 \rightarrow Z\chi_1^0)$ . Spectra are calculated with SUSY soft mass parameters  $M_0 = 2$  TeV,  $\tan\beta = 10$ ,  $m_A = 2$  TeV,  $A_0 = 2.5$  TeV,  $M_1 = 200$  GeV,  $M_3 = 2$  TeV using SOFTSUSY v3.3.8 [109], and decay tables are calculated with SUSYHIT v1.3 [110–113]. The upper panels have wino-like NLSPs, with  $M_2 < \mu$ . Because of mixing with the bino, the mass splitting between the NLSP and LSP is not large for small  $M_2$ , but once the mass splitting exceeds the Higgs threshold, the branching fraction for  $\chi_2^0 \rightarrow h\chi_1^0$  easily dominates over  $Z\chi_1^0$ . Similarly, the bottom panels have Higgsino-like NLSPs, with  $\mu \lesssim M_2$  in the lower left panel and  $\mu < M_2$  in the lower right panel. Since the Higgs decay channel is kinematically open for this entire parameter range, we see from the lower left panel that it is favored compared to the  $Z$  channel. The lower right panel has the same behavior except for low  $\mu$ , where a level-crossing occurs and the different sign in the  $\chi_2^0$  gauge eigenstate composition leads a dominant  $Z$  decay to the LSP. We can see the complementary nature of exotic production probes and multilepton searches in this scenario, whose sensitivities are driven by  $\text{Br}(\chi_2^0 \rightarrow h\chi_1^0)$  and  $\text{Br}(\chi_2^0 \rightarrow Z\chi_1^0)$ . For all of these points, the associated chargino  $\chi_1^\pm$  is nearly mass-degenerate with  $\chi_2^0$  and decays to  $W^\pm\chi_1^0$  (sometimes via an off-shell  $W^*$ ) 100% of the time.

In addition, the production cross sections for  $pp \rightarrow \chi_1^\pm\chi_2^0$  can be large, which we show in Fig. 3 as a function of the same mass parameters as before: either  $M_2$  ( $\mu$  fixed to 800 GeV or 2 TeV) or  $\mu$  ( $M_2$  fixed to 500 or 2 TeV). These cross sections are calculated using PROSPINO v.2.1 [114]. Recall that  $Wh$  production in the SM is 0.6860 pb (for  $m_h = 126$  GeV), so the contamination fraction for  $Wh + \text{MET}$  relative to  $Wh$  in the SM can be order 1 or larger.

### A. Benchmark models for exotic production

We will study higgsino-like NLSPs and wino-like NLSPs, keeping in mind from Fig. 2 that multilepton searches give indirect constraints on these exotic Higgs production models. We choose benchmark points as shown in Table II. The mass spectra are calculated using SOFTSUSY

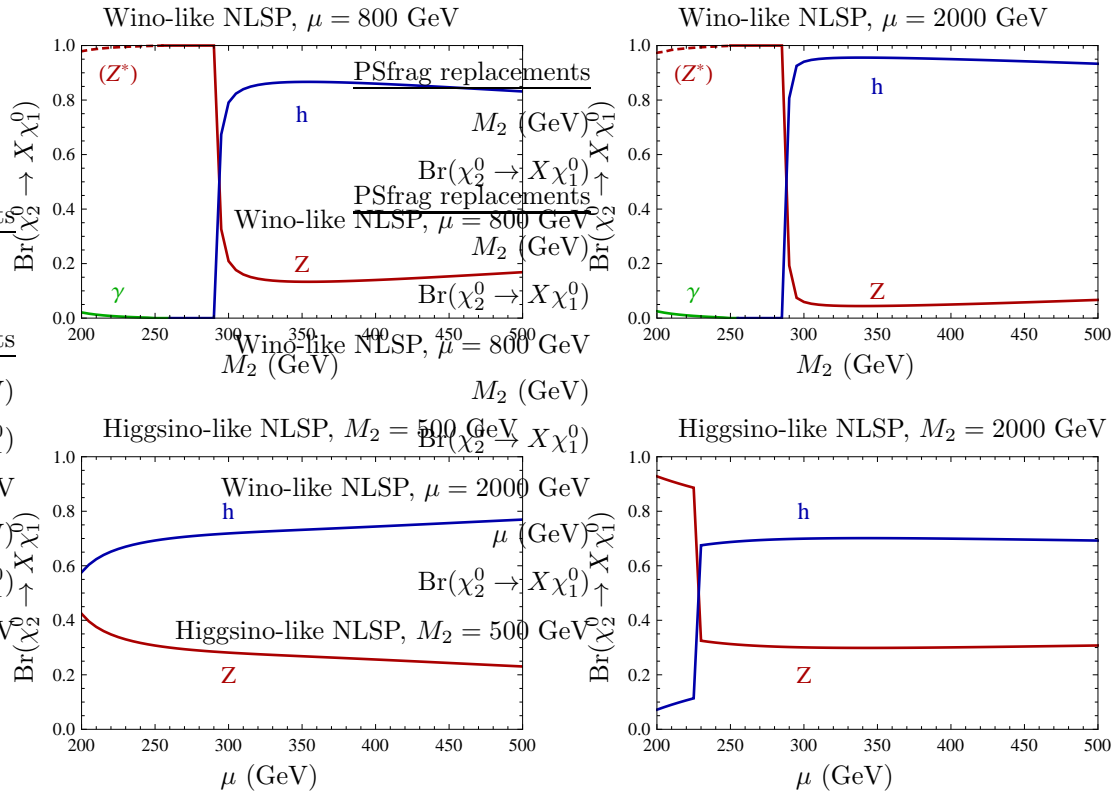


FIG. 2. Relevant branching fractions of  $\chi_2^0 \rightarrow h\chi_1^0$  (blue),  $Z\chi_1^0$  (red),  $\gamma\chi_1^0$  (green). Each panel uses SUSY soft mass parameters  $M_0 = 2$  TeV,  $\tan\beta = 10$ ,  $m_A = 2$  TeV,  $A_0 = 2.5$  TeV,  $M_1 = 200$  GeV,  $M_3 = 2$  TeV at the mSUGRA scale.

v3.3.8 [109], and branching fractions are calculated with SUSYHIT v1.3 [110–113]. We use PROSPINO v.2.1 [114] for the next-to-leading order (NLO) cross sections at 8 TeV LHC, and relic abundance is calculated using MICROMEGAS v.3.6.7 [115]. We now detail the model phenomenology and current constraints from direct searches, multilepton studies, and dedicated  $Wh$ +MET searches.

First, the model benchmarks have heavy scalars and a gluino in the TeV to multi-TeV range, which satisfy the limits on squarks and gluino production in jets + MET final states. Moreover, the radiative corrections induced by the multi-TeV stops and gluino drive the lightest SM-like Higgs mass to 125.5 GeV within theory uncertainty. Separately, the relic abundance of the bino-like LSP satisfies constraints on  $\Omega h^2 = 0.1198 \pm 0.0026$  [116] and the most recent direct detection constraints on dark matter-nucleon cross sections [117], and so the LSP is a suitable dark matter candidate. Furthermore, the invisible decay of  $h \rightarrow \chi_1^0\chi_1^0$  is suppressed below current constraints. The remaining flavor constraints, direct searches for the heavy Higgs sector and sleptons are also

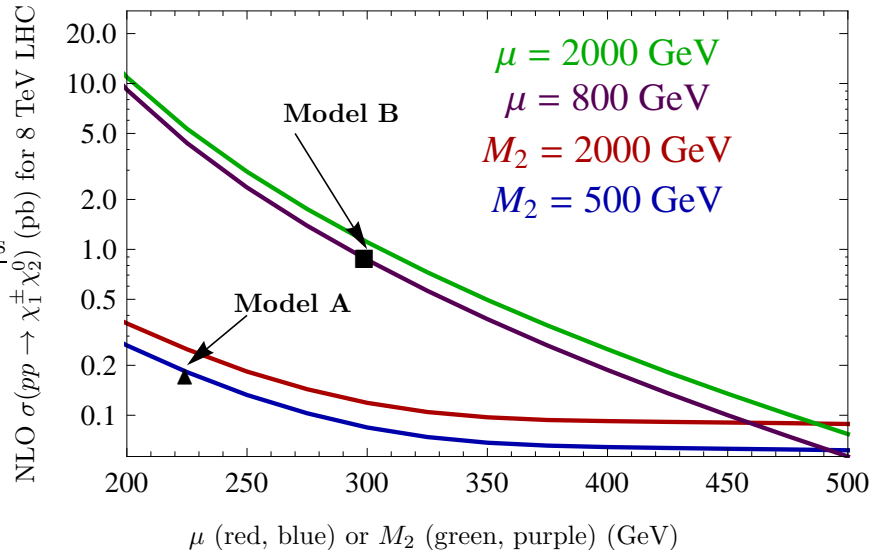


FIG. 3. Cross sections for  $pp \rightarrow \chi_1^\pm \chi_2^0$  (pb) at 8 TeV LHC as labeled. Note the horizontal axis is either  $\mu$  or  $M_2$  according to the relevant curve.

easily satisfied by the mass decoupling of the spectra. These two models, although fine-tuned, exemplify the simplified model [118] attitude. Here, the LHC accessible electroweak gaugino states and their interesting phenomenology can be isolated and discussed separately from the model constraints on the full theory, as demonstrated by explicit construction. As a corollary, this example of exotic production of the Higgs introduces observable deviations in Higgs physics while staying within the MSSM decoupling limit, which only constrains SM Higgs production and decay rates!

We can see that Model A has a dominantly Higgsino-like chargino-neutralino pair at about 215 GeV (in this model,  $\chi_3^0$  has a mass of 239 GeV), while Model B has a dominantly Wino-like chargino-neutralino pair at 191 GeV. As previewed in Figs. 2 and 3, both scenarios have a suppressed  $WZ + \text{MET}$  cascade decay rate, which is probed in multilepton analyses aimed at the leptonic decays of the gauge bosons. Comparing to multilepton event searches [119–123] and rescaling the limits by the appropriate  $\chi_2^0 \rightarrow Z\chi_1^0$  branching fraction, we see both benchmarks satisfy the current multilepton constraints. Moreover, direct chargino pair production searches, interpreted without intermediate sleptons in the cascade decay, are also satisfied, since the current limits are not yet sensitive to these cross sections [122].

Separately, the  $Wh + \text{MET}$ ,  $h \rightarrow bb$  or same-sign dilepton +  $jj(j) + \text{MET}$  searches [124, 125] are insensitive to our model benchmarks, since both models lie relatively close to the Higgs mass difference line in the  $\chi_1^\pm/\chi_2^0$  mass vs.  $\chi_1^0$  mass plane. In these searches, the expected SM  $Wh$

Parameter	Model A	Model B
$M_0$	2000	2000
$\tan \beta$	10	10
$m_A$	2000	2000
trilinear $A_0$	2500	2500
$M_1$	200	200
$M_2$	500	300
$M_3$	2000	2000
$\mu$	225	800
$\chi_1^\pm$ mass	213 GeV	191 GeV
$\chi_2^0$ mass	215 GeV	191 GeV
$\chi_1^0$ mass	57.8 GeV	61.5 GeV
$\text{BR}(\chi_2^0 \rightarrow h\chi_1^0)$	66.2%	79.1%
$\text{BR}(\chi_2^0 \rightarrow Z\chi_1^0)$	33.8%	20.9%
$\text{BR}(\chi_2^\pm \rightarrow W^\pm\chi_1^0)$	100%	100%
$\sigma(\chi_1^+\chi_2^0)$	0.126	0.622
$\sigma(\chi_1^-\chi_2^0)$	0.058	0.295
$\Omega h^2$	0.0211	0.117
$\sigma_{SI,p}$	$7.265 \times 10^{-10}$	$2.193 \times 10^{-11}$
$\sigma_{SD,p}$	$5.858 \times 10^{-5}$	$3.341 \times 10^{-7}$
$\sigma_{SI,n}$	$7.442 \times 10^{-10}$	$2.251 \times 10^{-11}$
$\sigma_{SD,n}$	$4.488 \times 10^{-5}$	$2.624 \times 10^{-7}$
$\text{Br}(h \rightarrow \chi_1^0\chi_1^0)$	0.035	$3.60 \times 10^{-5}$

TABLE II. Model parameters for benchmark models A and B. Masses are in GeV, cross sections are in pb.

contribution is cut from the analyses via a hard transverse mass cut, rendering them insensitive to the Higgs mass difference line where the cascade decay of the heavy neutralino produces a very weakly boosted Higgs boson. Hence, we can additionally motivate our analyses of the Higgs discovery modes as probing this complementary part of parameter space where the previous  $Wh + \text{MET}$  analyses do not have sensitivity. The two benchmarks are thus illustrative in understanding the effect of changing the  $\chi_2^0 - \chi_1^0$  mass difference in order to interpolate between the above searches,

which are sensitive to large mass splittings and moderately boosted Higgses, versus the SM Higgs analyses, which are probing the non-boosted regime of exotic production.

#### IV. EFFECTS ON CURRENT HIGGS ANALYSES FROM EXOTIC PRODUCTION

Having established our benchmark models, we proceed with quantifying how they can be probed in the Higgs discovery analyses. We perform Monte Carlo simulations implementing the cut-and-count analyses of ATLAS [4–6] and CMS [1–3]. This will determine signal efficiencies for our benchmark exotic modes of the SM-like Higgs. We will then discuss the calculated efficiencies, make comparisons to extrapolated SM signal efficiencies, and the necessary probes to distinguish exotic and SM production modes. We neglect the effect of these exotic production benchmarks on the data-driven background control regions and instead only focus on signal regions.

Event samples are generated using MADGRAPH5 v1.5.7 [126] with the CTEQ6L1 PDFs [127]. Each event is passed through PYTHIA v6.4.20 [128] for showering and hadronization. No detector simulation is used, but we do not expect it to significantly change the results, because the final states are high resolution channels (mainly photons and leptons) and the main cuts of the analysis that define the signal region are driven by these well-measured objects.

We use the cut and count analyses for the main Higgs discovery modes:  $h \rightarrow \gamma\gamma$ ,  $h \rightarrow ZZ^* \rightarrow 4\ell$ , and  $h \rightarrow WW^* \rightarrow \ell\nu\ell\nu$ , with  $\ell = e, \mu$ . In both Tables III and IV, the signal categorization efficiencies are given relative to the Higgs rate to the specified final state, except for the  $WW^*$  efficiency, which uses the Higgs rate  $h \rightarrow WW^* \rightarrow (\ell + \tau)\nu(\ell + \tau)\nu$ , to account for the subleading contribution from leptonic decays of  $\tau$ s. Numbers of expected events in the  $\gamma\gamma$ , for example, are then given by  $\sigma(pp \rightarrow \chi_1^\pm \chi_2^0) \times \text{Br}(\chi_1^+ \rightarrow W^+ \chi_1^0) \times \text{Br}(\chi_2^0 \rightarrow h \chi_1^0) \times \text{Br}_{SM}(h \rightarrow \gamma\gamma) \times \epsilon_{\gamma\gamma}$ , where  $\epsilon_{\gamma\gamma}$  is the appropriate category from the table. By design,  $\epsilon$  is the same as defined in Eq. (1), whereby all Higgs branching fractions are accounted for separately. Note that since our production mode has an extra  $W$  boson, we generate two orthogonal datasets for the  $WW^*$  analysis: (1)  $W \rightarrow \text{anything}$ ,  $h \rightarrow \ell\nu\ell\nu$ , and (2)  $W \rightarrow \ell\nu$ ,  $h \rightarrow \ell\nu jj$  with  $\ell = e, \mu$ , or  $\tau$ , since each could contribute to the  $\ell\nu\ell\nu$  final state. We combine the resulting separate signal efficiencies, appropriately normalized to the  $h \rightarrow (\ell + \tau)\nu(\ell + \tau)\nu$  rate. The ATLAS  $\gamma\gamma$  high-mass two-jet category combines the original orthogonal “loose” and “tight” categorizations. We only implement the gluon fusion targeted 0–jet and 1–jet search from the original CMS  $WW$  analysis, since the 2–jet analysis has limited statistical significance.

While most of the analyses have included selection efficiency tables for identification and re-

Analysis	Category	Model A	Model B
$\gamma\gamma$	Lepton	6.3%	6.6%
	MET significance	28.2%	22.7%
	Low-mass two-jet	1.4%	1.9%
	High-mass two-jet	0.2%	0.2%
	Untagged	9.1%	14.0%
$ZZ^*$	ggF-like	21.5%	21.4%
	VBF-like	0.2%	0.2%
	VH-like	7.1%	7.1%
$WW^*$	$N_{\text{jet}} = 0$	1.6%	1.7%
	$N_{\text{jet}} = 1$	3.4%	3.1%
	$N_{\text{jet}} \geq 2$	<0.1%	<0.1%

TABLE III. Signal categorization efficiencies for ATLAS  $\gamma\gamma$ ,  $ZZ^* \rightarrow 4\ell$ , and  $WW^* \rightarrow \ell\nu\ell\nu$  analyses. The  $WW^*$  rows sum the two orthogonal signal generation samples of  $Wh\chi_1^0\chi_1^0$ ,  $h \rightarrow \ell\nu\ell\nu$  ( $\ell = e, \mu, \tau$ ),  $W \rightarrow$  anything, and  $Wh\chi_1^0\chi_1^0$ ,  $W \rightarrow \ell\nu$ ,  $h \rightarrow \ell\nu jj$ , as described in the main text.

construction of signal objects, the ATLAS  $ZZ^*$  analysis only provides aggregate signal efficiencies. These are organized according to lepton final state and have expected signal reconstruction efficiencies for a 125 GeV Higgs produced in the SM as 39% for  $4\mu$ , 26% for  $2e2\mu$  and  $2\mu2e$ , and 19% for  $4e$ . We incorporate these efficiencies into our analysis by simulating gluon fusion production with a  $h + 0/1j$  matched sample and calculating the appropriate lepton category-specific reweighting factors. We apply these reweighting factors to account for identification and reconstruction efficiencies in our mock up of the ATLAS  $ZZ^*$  analysis, assuming these additional efficiencies only depend on lepton category and have no dependence on kinematics. As a cross check of this ad hoc procedure, we see our exotic NP efficiencies do mimic the extrapolated ATLAS SM  $Wh + Zh$  efficiencies shown Table VI of Sec. A. Namely, we see that the ggF-like, VBF-like, and VH-like categorization of  $Wh + Zh$  production are 22.4%, 0.3%, and 4.8%, respectively, which roughly follow our calculated NP efficiencies.

We can see that our two benchmarks have very similar signal categorization efficiencies from the cut and count Higgs analyses, with the notable exception of the MET categorization in the diphoton analyses. As expected, the larger mass splitting between  $\chi_2^0$  and  $\chi_1^0$  in Model A leads to a larger MET signal efficiency than that for Model B. With even heavier parent particles, the

Analysis	Category	Model A	Model B
$\gamma\gamma$	Muon	5.2%	5.1%
	Electron	5.1%	5.1%
	Dijet tight	0.1%	0.1%
	Dijet loose	0.3%	0.3%
	$E_T$ miss	26.7%	16.8%
	Untagged	20.2%	32.5%
$ZZ^*$	Category 1, $N_{\text{jet}} \leq 1$	22.1%	22.9%
	Category 2, $N_{\text{jet}} \geq 2$	11.6%	10.8%
$WW^*$	0-jet	0.3%	0.4%
	1-jet	1.0%	1.2%

TABLE IV. Signal categorization efficiencies for CMS  $\gamma\gamma$ ,  $ZZ^* \rightarrow 4\ell$ , and  $WW^* \rightarrow \ell\nu\ell\nu$  analyses.  $WW^*$  signal efficiencies are calculated the same as Table III.

MET efficiency will continue to grow and the Higgs would become more boosted, giving us a smooth transition from these SM-focused analyses and the dedicated boosted Higgs analyses. If we kept the mass splitting between the parent particles and the LSP constant and simply raised all masses together, however, we expect these efficiency tables to be largely unchanged. These orthogonal directions in this simplified model space can be explored simultaneously with a robust two-dimensional efficiency matrix, which we reserve for future work.

We remark that besides the low (targeting hadronic  $W$  and  $Z$  candidates) and high (targeting VBF forward jets) dijet cuts and the MET categorization, the remaining signal categories are simply multiplicity bins, and hence do not probe the different kinematics of the Higgs production mechanisms. On the other hand, differential distributions, especially in these well-measured, high-resolution leptonic and diphoton decay modes, would readily show signatures of exotic production modes: heavy particles cascade decaying to Higgses would show up as an edge feature in the  $p_T$  distribution of Higgs candidates, for example.

Using rates, however, we see that the most striking difference between our exotic production mode and the SM production modes lies in the MET bin efficiency. Comparing to Tables V and VIII, the only significant contribution to the MET category in the SM comes from  $Wh$  or  $Zh$  production with  $W \rightarrow \ell\nu$  or  $Z \rightarrow \nu\nu$ . These branching fractions suppress the MET categorization for such production modes by about 1/3 or 1/5. On the other hand, every event from  $\chi_1^\pm \chi_2^0$  production

gives rise to two escaping LSPs, and thus no invisible branching fraction suppression arises. Even with these large MET efficiencies, the benchmarks are, however, allowed from current data, since both the ATLAS  $\gamma\gamma$  analysis and the CMS mass-fit multivariate analysis have larger MET counts compared to expectation. For instance, ATLAS intriguingly identifies 8 MET significance-tagged events in data compared to 4 expected from background and 1.2 expected from SM signal [4]. Apart from rate, however, the MET distributions of our new physics benchmarks are very similar to the  $Wh$ ,  $W \rightarrow \ell\nu$  and  $Zh$ ,  $Z \rightarrow \nu\nu$  distributions, as shown in Fig. 4. Disentangling whether the MET associated with the Higgs has non-SM contributions will be difficult unless the MET distribution is strikingly different or we have high statistics. Nevertheless, the possibility that Higgs bosons are produced in association with dark matter candidates lends urgency to the need for the experiments to publish the MET distributions of their Higgs events.

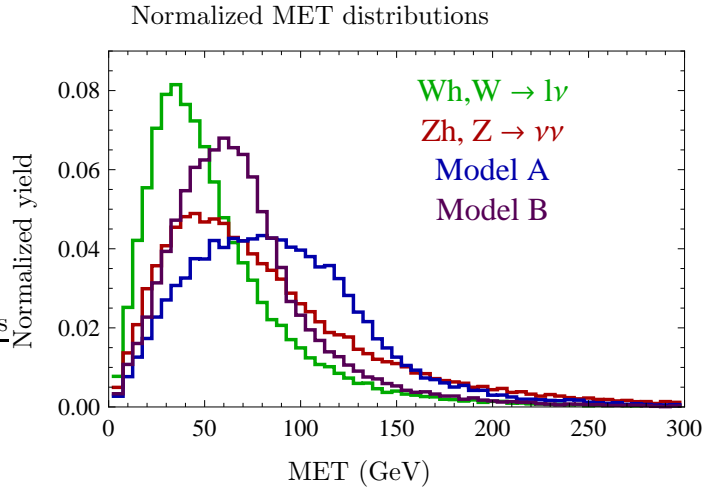


FIG. 4. Truth-level MET distributions in the ATLAS analysis of the  $\gamma\gamma$  channel for SM Higgs production via  $Wh$ ,  $W \rightarrow \ell\nu$  (green) and  $Zh$ ,  $Z \rightarrow \nu\nu$  (red), as well as exotic production benchmarks Model A (blue) and B (purple).

Since the diphoton analyses from both collaborations operate as inclusively as possible, most events that satisfy the Higgs candidate selection end up tagged, with “Untagged” being the catch-all category. This is notable because the SM gluon fusion production rate has the largest theory uncertainty (see Table I, although recent progress has been made at improving the fixed order calculation [129]). Hence, adopting a pessimistic perspective, any new physics exotic production that fails the checks for leptons, MET, and high and low two-jet mass windows will readily contaminate the untagged category, which may not register as significant given gluon fusion uncertainties. Nevertheless, further kinematic checks on  $p_T$  and  $\eta$  of the Higgs candidate could show striking

differences from SM expectations, which is again motivation to publish differential distributions for Higgs signal data.

The simplest perturbation to realize a model along these lines would be to allow for  $R$ -parity violation in our benchmarks, whereby the two LSPs could then decay promptly into three jets. Then the MET efficiency would likely drop to a negligible percentage and would instead flow down into the untagged category. The prospects for disentangling such an  $R$ -parity violating exotic production mode for the Higgs are dim unless further kinematic information is made available. We again emphasize that the Higgs  $p_T$  and MET and jet and lepton kinematics and multiplicities are critical distributions to publish and will serve well in distinguishing exotic from SM production modes.

Finally, we could proceed with a rate analysis based on the efficiencies in Tables III and IV and the extracted SM signal efficiencies in Sec. A following the observed number of events in each analysis and using Eq. (1). This style of rate analysis, which was similarly noted in [130], would detail the possible flat directions in trading one production mode for another. We want to go further, however, by convolving the Higgs couplings into the fit with the exotic production signal efficiencies. This is reserved for future work.

## V. CONCLUSION

We conclude by highlighting the main points of our analysis. We explored the phenomenology of exotic production of the SM-like Higgs. We find that new production modes for the Higgs are motivated from new physics models but are currently untested by the experimental rate results. Coupling measurements of the Higgs are currently interpreted in limited scenarios that exclude the possibility of new production modes. Since the kinematics and efficiencies of exotic production cannot be captured by a naive rescaling of the signal strength of SM production modes, such exotic production effects are not captured in the current Higgs coupling measurements. Moreover, using signal strengths of SM production modes to characterize the Higgs signal does not capture the full breadth of new phenomena possibly present in Higgs data, since SM signal efficiencies are held fixed. In particular, even the multidimensional coupling space explored in current Higgs fits cannot accommodate an exotic production mechanism. For example, if an excess of MET-tagged events were observed without observing corresponding dileptonic  $Z$  or a semileptonic  $W$  excesses, then the signal cannot be accommodated with simple variations of the  $Z$  or  $W$  coupling to the Higgs.

We have detailed the need for dedicated probes of exotic production. The narrow intrinsic

Higgs width, along with the new CMS bound on the Higgs width [58], and the SM expectation that it is a pure scalar, afford us to factorize production from decay. Searches for exotic decays typically require many new analyses, each targetting a new final state. On the other hand, probes of exotic production can be done with minimal modification to current analyses, especially those with well-identified Higgs candidates. In this vein, we highlighted the  $\gamma\gamma$ ,  $ZZ^*$ , and  $WW^*$  analyses as particularly relevant for further experimental study to detail the kinematics and multiplicities of objects produced in association with the Higgs, as well as kinematics of the Higgs candidate itself. In particular, MET distributions,  $p_T$  and  $\eta$  distributions are highly relevant for disentangling amongst possible competing production modes.

We have focused on chargino-neutralino cascade decays in the MSSM as benchmark examples of exotic production. By adjusting the mass splitting between the heavy parent particles and the LSP close to the Higgs mass, we have shown the complementary nature of the Higgs discovery analyses and dedicated SUSY searches in probing this simplified model space. From rate information alone, probing these benchmarks is difficult, relying only on the limited statistical power of MET-tagged Higgs events. Furthermore, allowing the LSPs to decay via  $R$ -parity violating couplings would drastically dilute the MET efficiency, making this exotic production mode very difficult to distinguish from SM  $Wh$  production. This motivates the need to go beyond rate information to explore exotic Higgs production and lends urgency to publish differential distributions in high resolution Higgs final state analyses. In particular, the  $R$ -parity violating version of Models A and B would be expected to introduce a flat direction in a combined fit to SM  $Wh$  and exotic production rates. Constructing models that mimic other SM production modes and hence introduce further flat directions is reserved for future work. Again, lifting these flat directions requires going beyond fitting for rates and instead fitting shapes of differential distributions.

In the end, we have broadened the range of possibilities for the next set of studies of Higgs data, focusing on how to construct and probe new production modes of the Higgs. Future work will focus on exploring how Higgs coupling fits should be expanded to include the possibility of exotic production modes. We will also further discuss the role of differential distributions in distinguishing various model classes of exotic production.

#### ACKNOWLEDGEMENTS

The author is grateful to Prateek Agrawal, Wolfgang Altmannshofer, Bogdan Dobrescu, Paddy Fox, Claudia Frugiuele, Roni Harnik, and Joe Lykken for useful discussions. Fermilab is operated

by Fermi Research Alliance, LLC under Contract No. De-AC02-07CH11359 with the United States Department of Energy.

### Appendix A: Extrapolated efficiencies

In this Appendix, we provide extrapolated experimental efficiencies based on the expected Higgs signal sensitivity of each ATLAS and CMS  $\gamma\gamma$ ,  $ZZ^* \rightarrow 4\ell$ ,  $WW^* \rightarrow \ell\nu\ell\nu$  analysis. Exact references are provided in each table caption.

	ggF	VBF	WH	ZH	$t\bar{t}H$
$N_{\text{events}}$ for $20.7 \text{ fb}^{-1}$	888.2	73.5	31.9	18.9	5.9
Lepton	0.0%	0.0%	5.3%	2.2%	8.5%
$E_T$ miss significance	0.0%	0.0%	1.3%	3.0%	2.4%
Low-mass two-jet	0.2%	0.0%	2.9%	2.9%	0.0%
Tight high-mass two-jet	0.2%	8.0%	0.0%	0.0%	0.0%
Loose high-mass two-jet	0.3%	3.7%	0.0%	0.0%	0.0%
Untagged	36.0%	25.8%	21.9%	22.2%	17.0%

TABLE V. Efficiency table for the ATLAS  $\gamma\gamma$  analysis derived from Table 5 of Ref. [30]. The mass window, centered at 126.5 GeV, is expected to contain 90% of the signal.

	ggF+ $t\bar{t}H$	VBF	WH+ZH
$N_{\text{events}}$ for $20.7 \text{ fb}^{-1}$	50.8	4.1	2.8
ggF-like	26.6%	19.3%	23.0%
VBF-like	0.6%	10.5%	0.4%
VH-like	0.1%	0.0%	5.0%

TABLE VI. Efficiency table for the ATLAS  $ZZ^*$  analysis derived from Table 2 of Ref. [5], with  $m_H = 125$  GeV.

	Signal
$N_{\text{events}}$ for $20.7 \text{ fb}^{-1}$	11029
0-jet	0.907%
1-jet	0.372%
$\geq 2$ -jet	0.099%

TABLE VII. Efficiency table for the ATLAS  $WW^*$  analysis derived from Table 9 of Ref. [30], with  $m_H = 125.5 \text{ GeV}$ . Event counts are given in the transverse mass region  $0.75m_H < m_T < m_H$  for  $N_{\text{jet}} \leq 1$  and  $m_T < 1.2m_H$  for  $N_{\text{jet}} \geq 2$ . Note here that we normalized the  $h \rightarrow WW^* \rightarrow \ell\nu\ell\nu$  rate to include  $\ell = e, \mu, \tau$ .

	ggF	VBF	VH	$t\bar{t}H$
$N_{\text{events}}$ for $19.6 \text{ fb}^{-1}$	861.1	70.5	50.0	5.8
Muon	0.0%	$< 0.1\%$	2.2%	5.0%
Electron	$< 0.1\%$	$< 0.1\%$	1.4%	3.1%
Dijet tight	0.2%	10.3%	$< 0.1\%$	0.2%
Dijet loose	0.6%	8.3%	0.4%	1.0%
$E_T$ miss	$< 0.1\%$	$< 0.1\%$	2.2%	3.4%
Untagged combined	38.3%	25.7%	31.1%	32.9%

TABLE VIII. Efficiency table for the CMS  $\gamma\gamma$  analysis derived from Table 5 of Ref. [1], which details the mass-fit MVA analysis, assuming a signal  $m_H = 125 \text{ GeV}$ .

	ggF	VBF	WH	ZH	$t\bar{t}H$
$N_{\text{events}}$ for $5.1 \text{ fb}^{-1} + 19.6 \text{ fb}^{-1}$	60.9	5.0	2.2	1.3	0.4
0/1-jet	25.3%	14.0%	12.6%	16.1%	0.0%
Dijet	2.6%	17.3%	9.5%	12.3%	20.3%

TABLE IX. Efficiency table for the CMS  $ZZ^*$  analysis derived from Table 5 of Ref. [2]. Results are integrated over the mass range 121.5 to 130.5 GeV and combine 7 and 8 TeV data. The signal uses  $m_H = 126 \text{ GeV}$ .

	ggF	VBF+VH
$N_{\text{events}}$ for $19.4 \text{ fb}^{-1}$	8852	1212
0-jet	1.62%	0.27%
1-jet	0.60%	0.79%

TABLE X. Efficiency table for the CMS  $WW^*$  analysis derived from Table 5 of Ref. [37], adopting the signal  $m_H = 125 \text{ GeV}$  row. Note here that we normalized the  $h \rightarrow \ell\nu\ell\nu$  rate to include  $\ell = e, \mu, \tau$ .

- 
- [1] S. Chatrchyan *et al.* (CMS Collaboration), (2013), CMS-PAS-HIG-13-001.
  - [2] S. Chatrchyan *et al.* (CMS Collaboration), (2013), arXiv:1312.5353 [hep-ex].
  - [3] S. Chatrchyan *et al.* (CMS Collaboration), (2013), CMS-PAS-HIG-13-003.
  - [4] G. Aad *et al.* (ATLAS Collaboration), (2013), ATLAS-CONF-2013-012.
  - [5] G. Aad *et al.* (ATLAS Collaboration), (2013), ATLAS-CONF-2013-013.
  - [6] G. Aad *et al.* (ATLAS Collaboration), (2013), ATLAS-CONF-2013-030.
  - [7] S. Dawson, A. Gritsan, H. Logan, J. Qian, C. Tully, *et al.*, (2013), arXiv:1310.8361 [hep-ex].
  - [8] A. Azatov, R. Contino, and J. Galloway, JHEP **1204**, 127 (2012), arXiv:1202.3415 [hep-ph].
  - [9] J. Espinosa, C. Grojean, M. Muhlleitner, and M. Trott, JHEP **1205**, 097 (2012), arXiv:1202.3697 [hep-ph].
  - [10] A. Azatov, R. Contino, D. Del Re, J. Galloway, M. Grassi, *et al.*, JHEP **1206**, 134 (2012), arXiv:1204.4817 [hep-ph].
  - [11] M. Klute, R. Lafaye, T. Plehn, M. Rauch, and D. Zerwas, Phys.Rev.Lett. **109**, 101801 (2012), arXiv:1205.2699 [hep-ph].
  - [12] D. Carmi, A. Falkowski, E. Kuflik, and T. Volansky, Frascati Phys.Ser. **57**, 315 (2013), arXiv:1206.4201 [hep-ph].
  - [13] K. Blum, R. T. D’Agnolo, and J. Fan, JHEP **1301**, 057 (2013), arXiv:1206.5303 [hep-ph].
  - [14] B. A. Dobrescu and J. D. Lykken, JHEP **1302**, 073 (2013), arXiv:1210.3342 [hep-ph].
  - [15] D. Carmi, A. Falkowski, E. Kuflik, T. Volansky, and J. Zupan, JHEP **1210**, 196 (2012), arXiv:1207.1718 [hep-ph].
  - [16] T. Plehn and M. Rauch, Europhys.Lett. **100**, 11002 (2012), arXiv:1207.6108 [hep-ph].
  - [17] A. David *et al.* (LHC Higgs Cross Section Working Group), (2012), arXiv:1209.0040 [hep-ph].
  - [18] T. Corbett, O. Eboli, J. Gonzalez-Fraile, and M. Gonzalez-Garcia, Phys.Rev. **D87**, 015022 (2013), arXiv:1211.4580 [hep-ph].
  - [19] G. Belanger, B. Dumont, U. Ellwanger, J. Gunion, and S. Kraml, Phys.Lett. **B723**, 340 (2013), arXiv:1302.5694 [hep-ph].
  - [20] A. Falkowski, F. Riva, and A. Urbano, JHEP **1311**, 111 (2013), arXiv:1303.1812 [hep-ph].
  - [21] P. P. Giardino, K. Kannike, I. Masina, M. Raidal, and A. Strumia, (2013), arXiv:1303.3570 [hep-ph].
  - [22] A. Djouadi and G. Moreau, (2013), arXiv:1303.6591 [hep-ph].
  - [23] T. Corbett, O. Eboli, J. Gonzalez-Fraile, and M. Gonzalez-Garcia, (2013), arXiv:1306.0006 [hep-ph].
  - [24] P. Artoisenet, P. de Aquino, F. Demartin, R. Frederix, S. Frixione, *et al.*, JHEP **1311**, 043 (2013), arXiv:1306.6464 [hep-ph].
  - [25] A. Pomarol and F. Riva, (2013), arXiv:1308.2803 [hep-ph].
  - [26] E. Boos, V. Bunichev, M. Dubinin, and Y. Kurihara, (2013), arXiv:1309.5410 [hep-ph].
  - [27] O. Stl and T. Stefaniak, (2013), arXiv:1310.4039 [hep-ph].

- [28] G. Aad *et al.* (ATLAS Collaboration), (2013), ATLAS-CONF-2013-014.
- [29] G. Aad *et al.* (ATLAS Collaboration), (2013), ATLAS-CONF-2013-034.
- [30] G. Aad *et al.* (ATLAS Collaboration), Phys.Lett. **B726**, 88 (2013), arXiv:1307.1427 [hep-ex].
- [31] S. Chatrchyan *et al.* (CMS Collaboration), (2013), CMS-PAS-HIG-13-005.
- [32] G. Aad *et al.* (ATLAS Collaboration), (2014), ATLAS-CONF-2014-010.
- [33] G. Aad *et al.* (ATLAS Collaboration), (2013), ATLAS-CONF-2013-040.
- [34] G. Aad *et al.* (ATLAS Collaboration), Phys.Lett. **B726**, 120 (2013), arXiv:1307.1432 [hep-ex].
- [35] G. Aad *et al.* (ATLAS Collaboration), (2013), ATLAS-CONF-2013-029.
- [36] G. Aad *et al.* (ATLAS Collaboration), (2013), ATLAS-CONF-2013-031.
- [37] S. Chatrchyan *et al.* (CMS Collaboration), (2013), arXiv:1312.1129 [hep-ex].
- [38] S. Chatrchyan *et al.* (CMS Collaboration), (2013), CMS-PAS-HIG-13-016.
- [39] G. Aad *et al.* (ATLAS Collaboration), (2013), ATLAS-CONF-2013-108.
- [40] S. Chatrchyan *et al.* (CMS Collaboration), (2014), arXiv:1401.5041 [hep-ex].
- [41] H.-L. Li, Z.-G. Si, X.-Y. Yang, Z.-J. Yang, and Y.-J. Zheng, Phys.Rev. **D87**, 115024 (2013), arXiv:1305.1457 [hep-ph].
- [42] V. Rentala, N. Vignaroli, H.-n. Li, Z. Li, and C. P. Yuan, Phys.Rev. **D88**, 073007 (2013), arXiv:1306.0899 [hep-ph].
- [43] G. Isidori and M. Trott, (2013), arXiv:1307.4051 [hep-ph].
- [44] S. Banerjee, S. Mukhopadhyay, and B. Mukhopadhyaya, (2013), arXiv:1308.4860 [hep-ph].
- [45] J. Gao, (2013), arXiv:1308.5453 [hep-ph].
- [46] A. Azatov and A. Paul, (2013), arXiv:1309.5273 [hep-ph].
- [47] C. Englert, M. McCullough, and M. Spannowsky, (2013), arXiv:1310.4828 [hep-ph].
- [48] F. Maltoni, K. Mawatari, and M. Zaro, (2013), arXiv:1311.1829 [hep-ph].
- [49] J. Huang, T. Liu, L.-T. Wang, and F. Yu, (2013), arXiv:1309.6633 [hep-ph].
- [50] D. Curtin, R. Essig, S. Gori, P. Jaiswal, A. Katz, *et al.*, (2013), arXiv:1312.4992 [hep-ph].
- [51] G. Aad *et al.* (ATLAS Collaboration), (2013), ATLAS-CONF-2013-011.
- [52] S. Chatrchyan *et al.* (CMS Collaboration), (2013), CMS-PAS-HIG-13-028.
- [53] S. Chatrchyan *et al.* (CMS Collaboration), (2013), CMS-PAS-HIG-13-013.
- [54] S. Chatrchyan *et al.* (CMS Collaboration), (2013), CMS-PAS-HIG-13-018.
- [55] F. Caola and K. Melnikov, Phys.Rev. **D88**, 054024 (2013), arXiv:1307.4935 [hep-ph].
- [56] J. M. Campbell, R. K. Ellis, and C. Williams, (2013), arXiv:1311.3589 [hep-ph].
- [57] J. M. Campbell, R. K. Ellis, and C. Williams, Phys.Rev. **D89**, 053011 (2014), arXiv:1312.1628 [hep-ph].
- [58] S. Chatrchyan *et al.* (CMS Collaboration), (2014), CMS-PAS-HIG-14-002.
- [59] S. Chatrchyan *et al.* (CMS Collaboration), (2013), CMS-PAS-HIG-13-025.
- [60] A. Datta, A. Djouadi, M. Guchait, and F. Moortgat, Nucl.Phys. **B681**, 31 (2004), arXiv:hep-ph/0303095 [hep-ph].

- [61] K. Huitu, R. Kinnunen, J. Laamanen, S. Lehti, S. Roy, *et al.*, Eur.Phys.J. **C58**, 591 (2008), arXiv:0808.3094 [hep-ph].
- [62] S. Gori, P. Schwaller, and C. E. Wagner, Phys.Rev. **D83**, 115022 (2011), arXiv:1103.4138 [hep-ph].
- [63] O. Stal and G. Weiglein, JHEP **1201**, 071 (2012), arXiv:1108.0595 [hep-ph].
- [64] J. M. Butterworth, A. R. Davison, M. Rubin, and G. P. Salam, Phys.Rev.Lett. **100**, 242001 (2008), arXiv:0802.2470 [hep-ph].
- [65] G. D. Kribs, A. Martin, T. S. Roy, and M. Spannowsky, Phys.Rev. **D81**, 111501 (2010), arXiv:0912.4731 [hep-ph].
- [66] G. D. Kribs, A. Martin, T. S. Roy, and M. Spannowsky, Phys.Rev. **D82**, 095012 (2010), arXiv:1006.1656 [hep-ph].
- [67] J. Gunion, H. Haber, R. M. Barnett, M. Drees, D. Karatas, *et al.*, Int.J.Mod.Phys. **A2**, 1145 (1987).
- [68] J. F. Gunion and H. E. Haber, Phys.Rev. **D37**, 2515 (1988).
- [69] A. Bartl, W. Majerotto, and N. Oshimo, Phys.Lett. **B216**, 233 (1989).
- [70] A. Djouadi, Y. Mambrini, and M. Muhlleitner, Eur.Phys.J. **C20**, 563 (2001), arXiv:hep-ph/0104115 [hep-ph].
- [71] M. A. Diaz and P. Fileviez Perez, J.Phys. **G31**, 563 (2005), arXiv:hep-ph/0412066 [hep-ph].
- [72] H. Baer, V. Barger, A. Lessa, W. Sreethawong, and X. Tata, Phys.Rev. **D85**, 055022 (2012), arXiv:1201.2949 [hep-ph].
- [73] D. Ghosh, M. Guchait, and D. Sengupta, Eur.Phys.J. **C72**, 2141 (2012), arXiv:1202.4937 [hep-ph].
- [74] A. Arbey, M. Battaglia, and F. Mahmoudi, (2012), arXiv:1212.6865 [hep-ph].
- [75] H. Baer, V. Barger, and D. Mickelson, Phys.Lett. **B726**, 330 (2013), arXiv:1303.3816 [hep-ph].
- [76] H. Baer, V. Barger, P. Huang, D. Mickelson, A. Mustafayev, *et al.*, (2013), arXiv:1306.2926 [hep-ph].
- [77] H. Baer, V. Barger, P. Huang, D. Mickelson, A. Mustafayev, *et al.*, (2013), arXiv:1306.3148 [hep-ph].
- [78] T. Han, T. Li, S. Su, and L.-T. Wang, JHEP **1311**, 053 (2013), arXiv:1306.3229 [hep-ph].
- [79] H. Baer, V. Barger, D. Mickelson, and X. Tata, (2013), arXiv:1306.4183 [hep-ph].
- [80] M. Berggren, F. Brummer, J. List, G. Moortgat-Pick, T. Robens, *et al.*, (2013), 10.1140/epjc/s10052-013-2660-y, arXiv:1307.3566 [hep-ph].
- [81] A. Bharucha, S. Heinemeyer, and F. Pahlen, Eur.Phys.J. **C73**, 2629 (2013), arXiv:1307.4237.
- [82] S. Gori, S. Jung, and L.-T. Wang, (2013), arXiv:1307.5952 [hep-ph].
- [83] B. Batell, S. Jung, and C. E. M. Wagner, (2013), 10.1007/JHEP12(2013)075, arXiv:1309.2297 [hep-ph].
- [84] T. Han, S. Padhi, and S. Su, (2013), arXiv:1309.5966 [hep-ph].
- [85] M. Berggren, T. Han, J. List, S. Padhi, S. Su, *et al.*, (2013), arXiv:1309.7342 [hep-ph].
- [86] M. R. Buckley, J. D. Lykken, C. Rogan, and M. Spiropulu, (2013), arXiv:1310.4827 [hep-ph].
- [87] A. Papaefstathiou, K. Sakurai, and M. Takeuchi, (2014), arXiv:1404.1077 [hep-ph].
- [88] S. Chatrchyan *et al.* (CMS Collaboration), (2013), arXiv:1312.3310 [hep-ex].
- [89] K. Howe and P. Saraswat, JHEP **1210**, 065 (2012), arXiv:1208.1542 [hep-ph].

- [90] K. Kumar, R. Vega-Morales, and F. Yu, *Phys.Rev.* **D86**, 113002 (2012), arXiv:1205.4244 [hep-ph].
- [91] S. Dittmaier *et al.* (LHC Higgs Cross Section Working Group), (2011), 10.5170/CERN-2011-002, arXiv:1101.0593 [hep-ph].
- [92] S. Dittmaier, S. Dittmaier, C. Mariotti, G. Passarino, R. Tanaka, *et al.*, (2012), 10.5170/CERN-2012-002, arXiv:1201.3084 [hep-ph].
- [93] S. Heinemeyer *et al.* (LHC Higgs Cross Section Working Group), (2013), 10.5170/CERN-2013-004, arXiv:1307.1347 [hep-ph].
- [94] P. Jaiswal, K. Kopp, and T. Okui, *Phys.Rev.* **D87**, 115017 (2013), arXiv:1303.1181 [hep-ph].
- [95] S. Chatrchyan *et al.* (CMS Collaboration), (2013), CMS-PAS-HIG-13-022.
- [96] S. Chatrchyan *et al.* (CMS Collaboration), (2013), CMS-PAS-HIG-13-011.
- [97] S. Chatrchyan *et al.* (CMS Collaboration), (2013), CMS-PAS-HIG-12-053.
- [98] S. Chatrchyan *et al.* (CMS Collaboration), (2013), CMS-PAS-HIG-13-009.
- [99] S. Chatrchyan *et al.* (CMS Collaboration), (2013), arXiv:1310.3687 [hep-ex].
- [100] S. Chatrchyan *et al.* (CMS Collaboration), (2013), CMS-PAS-HIG-13-017.
- [101] G. Aad *et al.* (ATLAS Collaboration), (2013), ATLAS-CONF-2013-075.
- [102] G. Aad *et al.* (ATLAS Collaboration), (2013), ATLAS-CONF-2013-079.
- [103] S. Chatrchyan *et al.* (CMS Collaboration), (2013), CMS-PAS-HIG-13-019.
- [104] S. Chatrchyan *et al.* (CMS Collaboration), (2013), CMS-PAS-HIG-13-015.
- [105] S. Chatrchyan *et al.* (CMS Collaboration), (2013), CMS-PAS-HIG-13-020.
- [106] G. Aad *et al.* (ATLAS Collaboration), (2013), ATLAS-CONF-2013-080.
- [107] F. Boudjema, G. Cacciapaglia, K. Cranmer, G. Dissertori, A. Deandrea, *et al.*, (2013), arXiv:1307.5865 [hep-ph].
- [108] G. Aad *et al.*, (2013), ATLAS-CONF-2013-072.
- [109] B. Allanach, *Comput.Phys.Commun.* **143**, 305 (2002), arXiv:hep-ph/0104145 [hep-ph].
- [110] A. Djouadi, M. Muhlleitner, and M. Spira, *Acta Phys.Polon.* **B38**, 635 (2007), arXiv:hep-ph/0609292 [hep-ph].
- [111] A. Djouadi, J.-L. Kneur, and G. Moultaka, *Comput.Phys.Commun.* **176**, 426 (2007), arXiv:hep-ph/0211331 [hep-ph].
- [112] A. Djouadi, J. Kalinowski, and M. Spira, *Comput.Phys.Commun.* **108**, 56 (1998), arXiv:hep-ph/9704448 [hep-ph].
- [113] M. Muhlleitner, A. Djouadi, and Y. Mambrini, *Comput.Phys.Commun.* **168**, 46 (2005), arXiv:hep-ph/0311167 [hep-ph].
- [114] W. Beenakker, M. Klasen, M. Kramer, T. Plehn, M. Spira, *et al.*, *Phys.Rev.Lett.* **83**, 3780 (1999), arXiv:hep-ph/9906298 [hep-ph].
- [115] G. Belanger, F. Boudjema, A. Pukhov, and A. Semenov, *Comput.Phys.Commun.* **185**, 960 (2014), arXiv:1305.0237 [hep-ph].
- [116] J. Beringer *et al.* (Particle Data Group), *Phys.Rev.* **D86**, 010001 (2012).

- [117] D. Akerib *et al.* (LUX Collaboration), (2013), arXiv:1310.8214 [astro-ph.CO].
- [118] D. Alves *et al.* (LHC New Physics Working Group), J.Phys. **G39**, 105005 (2012), arXiv:1105.2838 [hep-ph].
- [119] T. A. Aaltonen *et al.* (CDF Collaboration), Phys.Rev.Lett. (2013), arXiv:1309.7509 [hep-ex].
- [120] G. Aad *et al.* (ATLAS Collaboration), Phys.Rev. **D87**, 052002 (2013), arXiv:1211.6312 [hep-ex].
- [121] G. Aad *et al.* (ATLAS Collaboration), (2014), arXiv:1402.7029 [hep-ex].
- [122] G. Aad *et al.* (ATLAS Collaboration), (2013), ATLAS-CONF-2013-049.
- [123] S. Chatrchyan *et al.* (CMS Collaboration), (2013), CMS-PAS-SUS-13-006.
- [124] G. Aad *et al.* (ATLAS Collaboration), (2013), ATLAS-CONF-2013-093.
- [125] S. Chatrchyan *et al.* (CMS Collaboration), (2013), CMS-PAS-SUS-13-017.
- [126] J. Alwall, M. Herquet, F. Maltoni, O. Mattelaer, and T. Stelzer, JHEP **1106**, 128 (2011), arXiv:1106.0522 [hep-ph].
- [127] J. Pumplin, D. Stump, J. Huston, H. Lai, P. M. Nadolsky, *et al.*, JHEP **0207**, 012 (2002), arXiv:hep-ph/0201195 [hep-ph].
- [128] T. Sjostrand, S. Mrenna, and P. Z. Skands, JHEP **0605**, 026 (2006), arXiv:hep-ph/0603175 [hep-ph].
- [129] C. Anastasiou, C. Duhr, F. Dulat, E. Furlan, T. Gehrmann, *et al.*, (2014), arXiv:1403.4616 [hep-ph].
- [130] A. Djouadi, Eur.Phys.J. **C73**, 2498 (2013), arXiv:1208.3436 [hep-ph].